Global impact of atmospheric arsenic on health risk: 2005 to 2015

Lei Zhang[a], Yang Gao[a,b,1], Shiliang Wu[c,1], Shaoqing Zhang[d,e,f], Kirk R. Smith[g,h,1], Xiaohong Yao[a,b], and Huiwang Gao[a,b]

[a]Frontiers Science Center for Deep Ocean Multispheres and Earth System/Key Laboratory of Marine Environmental Science and Ecology, Ministry of Education, Ocean University of China, 266100 Qingdao, China; [b]Laboratory for Marine Ecology and Environmental Science, Qingdao National Laboratory for Marine Science and Technology, 266237 Qingdao, China; [c]Atmospheric Sciences Program, Michigan Technological University, Houghton, MI 49931; [d]Key Laboratory of Physical Oceanography, Ministry of Education/Institute for Advanced Ocean Study/Frontiers Science Center for Deep Ocean Multispheres and Earth System, Ocean University of China and Qingdao National Laboratory for Marine Science and Technology, 266100 Qingdao, China; [e]International Laboratory for High-Resolution Earth System Prediction, 266237 Qingdao, China; [f]College of Oceanic and Atmospheric Sciences, Ocean University of China, Qingdao 266100, China; [g]School of Public Health, University of California, Berkeley, CA 94720; and [h]Collaborative Clean Air Policy Centre, Delhi 110003, India

Contributed by Kirk R. Smith, April 14, 2020 (sent for review February 13, 2020; reviewed by Randall V. Martin and Hezhong Tian)

Arsenic is a toxic pollutant commonly found in the environment. Most of the previous studies on arsenic pollution have primarily focused on arsenic contamination in groundwater. In this study, we examine the impact on human health from atmospheric arsenic on the global scale. We first develop an improved global atmospheric arsenic emission inventory and connect it to a global model (Goddard Earth Observing System [GEOS]-Chem). Model evaluation using observational data from a variety of sources shows the model successfully reproduces the spatial distribution of atmospheric arsenic around the world. We found that for 2005, the highest airborne arsenic concentrations were found over Chile and eastern China, with mean values of 8.34 and 5.63 ng/m^3, respectively. By 2015, the average atmospheric arsenic concentration in India (4.57 ng/m^3) surpassed that in eastern China (4.38 ng/m^3) due to the fast increase in coal burning in India. Our calculation shows that China has the largest population affected by cancer risk due to atmospheric arsenic inhalation in 2005, which is again surpassed by India in 2015. Based on potential exceedance of health-based limits, we find that the combined effect by including both atmospheric and groundwater arsenic may significantly enhance the risks, due to carcinogenic and noncarcinogenic effects. Therefore, this study clearly implies the necessity in accounting for both atmospheric and groundwater arsenic in future management.

atmospheric arsenic | GEOS-Chem | cancer risk | noncarcinogenic effect

Elemental arsenic and many of its compounds are highly toxic pollutants in the environment. Arsenic ingestion or inhalation can lead to diseases including cardiovascular disease, skin cancer, respiratory cancer, and other diseases (1–3). Due to the toxicity of arsenic, a limit of 6 ng/m^3 was established for the atmospheric arsenic by the European Union (EU) (4), and the World Health Organization recommends keeping the arsenic concentrations in drinking water below 10 μg/L (5). Recent studies, however, have reported that high arsenic concentrations well above these threshold values are frequently observed in many parts of the world. For instance, the airborne concentrations of arsenic, which were found in particles, may exceed 20 ng/m^3 in Chile and China (6–8); arsenic concentrations more than 300 μg/L in groundwater were observed in multiple countries such as Bangladesh, Iran, Vietnam, and Pakistan (9–14).

Compared with air, many more studies have been published quantifying the health effect of arsenic from water [i.e., China (15, 16), Bangladesh (17, 18), India (19, 20), Iran (21, 22), and Pakistan (23, 24)]. For atmospheric arsenic, limited observation [i.e., over Beijing, China (25) and Agra, India (26)] indicates that the exceedance of the level recommended by the US Environmental Protection Agency (EPA) may lead to enhanced carcinogenic risk (CR) (27). The sparse observed information, however, is insufficient to support full examination of the health impact from atmospheric arsenic at a larger spatial scale, implicative of the necessity of applying models.

For instance, through evaluating the spatial characteristics of heavy metals such as arsenic in Italy based on the Flexible Air quality Regional Model, it can be inferred from Adani et al. (28) that the deficiency of arsenic emission inventory may greatly limit the model's ability to reproduce arsenic distributions. Wai et al. (29) was the first study to examine the global distribution of atmospheric arsenic. They used a global model (Goddard Earth Observing System [GEOS]-Chem) to simulate the transport and deposition of atmospheric arsenic and quantified the source–receptor relationships among various regions around the world. However, they did not carry out any analyses on the potential impacts on human health from atmospheric arsenic, and the emission inventory had many missing sources [i.e., Chinese industrial and household coal consumption, which was claimed to contribute substantially (30)]; a limited number of observations overall failed to support a thorough global evaluation of arsenic.

In this study, we first develop an updated and improved global arsenic emission inventory starting with that of Wai et al. (29) and implement the arsenic inventory in GEOS-Chem. We then conduct a more comprehensive evaluation of the model-simulated global distribution of atmospheric arsenic using all

Significance

Exposure to arsenic, a toxic pollutant widespread in air and water, has detrimental impacts on human health. Previous studies on arsenic pollution have primarily focused on groundwater arsenic, leaving the influence of atmospheric arsenic largely ignored. In this study, we have successfully simulated the distribution of atmospheric arsenic around the world and thoroughly examined the health impacts from atmospheric arsenic on a global scale. We find that the combined effect from arsenic in both atmosphere and groundwater may substantially aggravate both the carcinogenic and noncarcinogenic risks associated with arsenic pollution. Our results have important implications for developing effective strategies to mitigate the impacts on public health from arsenic pollution.

Author contributions: Y.G., S.W., and K.R.S. designed research; L.Z., Y.G., and S.W. performed research; L.Z., Y.G., S.Z., X.Y., and H.G. analyzed data; and L.Z., Y.G., S.W., S.Z., K.R.S., X.Y., and H.G. wrote the paper.

Reviewers: R.V.M., Washington University in St. Louis; and H.T., Beijing Normal University.

The authors declare no competing interest.

[1]To whom correspondence may be addressed. Email: yanggao@ouc.edu.cn, slwu@mtu.edu, or krksmith@berkeley.edu.

This article contains supporting information online at https://www.pnas.org/lookup/suppl/doi:10.1073/pnas.2002580117/-/DCSupplemental.

First published June 8, 2020.

of the available observational data. Finally, we examine the impacts on public health from atmospheric arsenic exposure and present the quantitative assessment of the health risk associated with atmospheric arsenic at the global scale.

Results

Model Evaluation. To examine the temporal trends in emissions and atmospheric loading of arsenic, we develop the arsenic emission inventory, with spatial distributions shown in *SI Appendix*, Fig. S3, and run the model for both 2005 and 2015. The method of developing arsenic emission inventory is detailed in *Materials and Methods*, with discussions of the contribution composition by different source categories, continents, and top 10 countries in *SI Appendix*, section 2 and Figs. S4 and S5. The emission comparison with a recent study of Zhu et al. (31) is also discussed in *SI Appendix*, section 2. We evaluate the model performance, with a focus on the model-simulated atmospheric concentration and deposition flux of arsenic, using all of the observational data we can obtain for various sites around the world. We take advantage of the European Monitoring and Evaluation Programme (EMEP) (ebas.nilu.no/default.aspx) and Interagency Monitoring of Protected Visual Environments (IMPROVE) (views.cira.colostate.edu/iwdw/), datasets for atmospheric arsenic concentrations over Europe and United States, respectively. The atmospheric arsenic concentration data for other regions and the arsenic deposition data are collected and compiled based on dozens of individual studies (Fig. 1 *E* and *F* and *SI Appendix*, Fig. S6), with details including observation period, location, and aerosol sample type listed in *SI Appendix*, Tables S1 and S2. In particular, for all of the observations mentioned above, the arsenic is mainly collected from the aerosol sample of particulate matter $(PM)_{2.5}$, with only seven studies (*SI Appendix*, Table S1) from PM_{10} or total suspended particles.

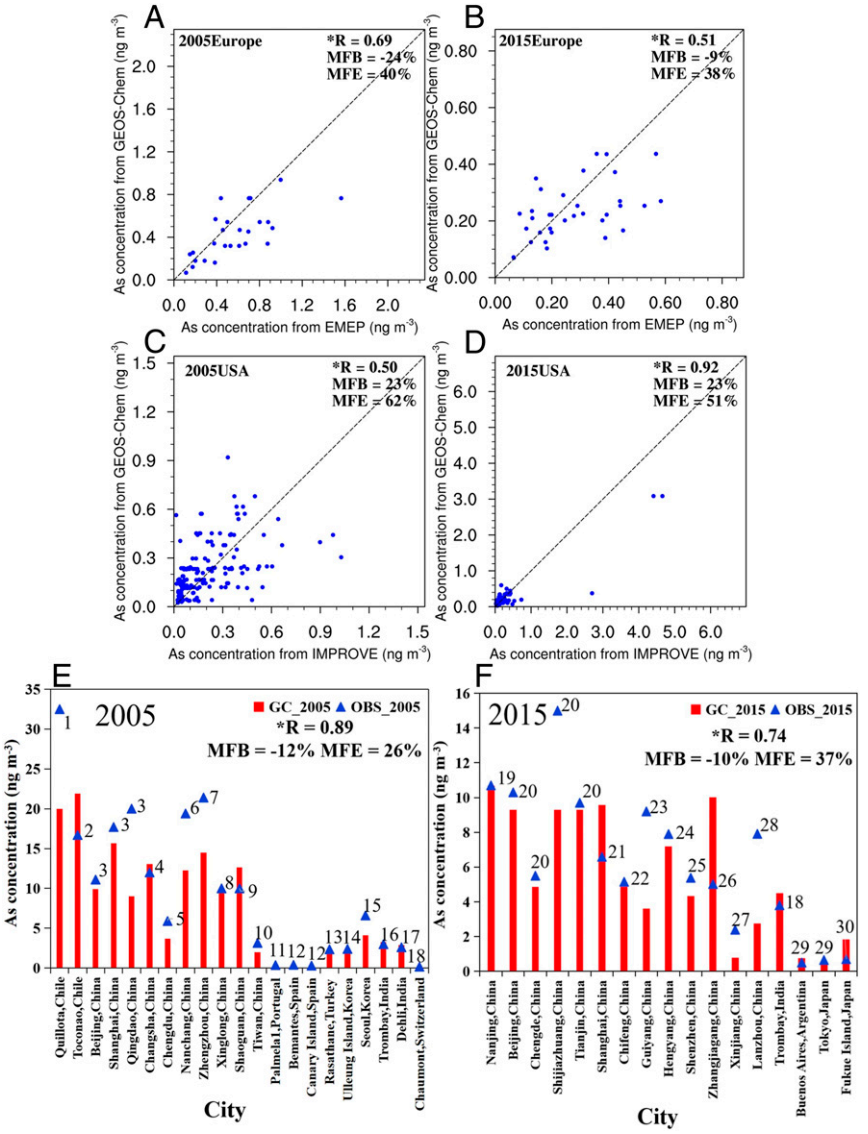

Fig. 1. Model-simulated atmospheric arsenic concentration compared with observational data at various sites from Europe (*A* and *B*), the United States (*C* and *D*), and other regions (*E* and *F*) for 2005 (*A*, *C*, and *E*) and 2015 (*B*, *D*, and *F*). The observational data for "other regions" were collected from individual studies with the specific references (shown in *SI Appendix*, Table S1) numbered as 1 to 30 adjacent to the data (triangles). The correlation coefficient *R*, marked with asterisks, indicating statistical significance at 95th level is shown in the upper right of each panel. MFB, mean fractional bias; MFE, mean fractional error.

The model-simulated atmospheric arsenic concentration and deposition flux at various sites are compared with corresponding data in Fig. 1 and *SI Appendix*, Fig. S6, respectively. For the two regions (the EU and the United States) where there are continuous data available, we calculate the annual mean concentrations, while for other sites (the specific locations are shown in *SI Appendix*, Fig. S7), we do the model–data comparison based on the measurement period for the data. Overall, the model results show reasonable agreement with observational data around the world. The mean fractional bias and mean fractional error, with equations shown in *SI Appendix*, section 3, calculated for the atmospheric arsenic concentrations over each region are always within 25 and 70%, satisfying the criteria proposed for $PM_{2.5}$ modeling by US EPA (32).

The Distribution of Atmospheric Arsenic Concentration and Its Variation in 2005 and 2015. The global distributions of atmospheric arsenic concentration simulated with the GEOS-Chem model are shown in Fig. 2. In both 2005 and 2015, there are large spatial variations in the atmospheric loading of arsenic, with Chile and China (in particular, eastern China) having the highest atmospheric arsenic concentrations. For instance, the mean concentrations over Chile and eastern China are 8.34 and 5.63 ng/m^3, respectively, in 2005, and these values become 8.68 and 4.38 ng/m^3, respectively, in 2015.

The high arsenic concentration in Chile reflects the strong arsenic emissions from copper smelting since Chile is the world's largest producer of copper (33). Total arsenic emissions from Chile appear relatively stable in the 2005 to 2015 decade with slight increases (*SI Appendix*, Fig. S8). As a consequence, we see slight increases (by 0.34 ng/m^3, equivalent to 4%) in the average atmospheric arsenic concentrations over Chile from 2005 to 2015(Fig. 2*C*), consistent with the overall increase of 8% in arsenic emission (*SI Appendix*, Fig. S8). The rate of arsenic concentration change in Chile is half of the emission variation, in general comparable with the majority of other regions albeit of differences of ratio (*SI Appendix*, Fig. S9), likely an effect of transport and enhanced deposition (*SI Appendix*, Fig. S10) in particular over Chile and the areas with emission increases (*SI Appendix*, Fig. S8). The average atmospheric arsenic concentration over eastern China has reduced by 22%, from 5.63 ng/m^3 in 2005 to 4.38 ng/m^3 in 2015 (Fig. 2*C*), largely driven by the efforts in controlling particulate matter emissions from industrial sources such as coal-fired power plants and boilers, which reduced arsenic emissions at the same time (34). It is also noteworthy that the arsenic concentration over southwestern China (SWC) shows an increase in 2015 in comparison with 2005, concomitant with the substantial increase of India. For instance, the mean arsenic concentration in India is 4.57 ng/m^3 in 2015, 65% higher than that in 2005 (2.77 ng/m^3), a result of dramatic increase in uncontrolled coal combustion (87%) in 2015 relative to 2005 (35). We carry out a sensitivity test and confirm that 30 to 70% of the increase over SWC (i.e., Tibet Plateau area) was contributed by India (*SI Appendix*, Fig. S11).

The most striking increment of arsenic concentration in 2015, relative to 2005, is located over the junction of northeastern India, Bangladesh, and Nepal, which thereby leads to high arsenic deposition over this area, and the descriptions of arsenic deposition are in *SI Appendix*, section 4 and Fig. S10. The atmospheric arsenic deposition in some areas may apparently be connected to groundwater levels, as in Brazil (36). Interestingly, there have long been serious concerns of arsenic pollution in groundwater in this region. For example, sizable effect on early pulmonary effects was found by Smith et al. (37) and considerably large numbers of arsenicosis as well as arsenic-related cancers: that is, 1.85 million cases of arsenicosis (both hyperpigmentation and keratosis), 128,000 cases of skin cancer, and fatalities due to internal cancers [table 2 from Yu et al. (38)].

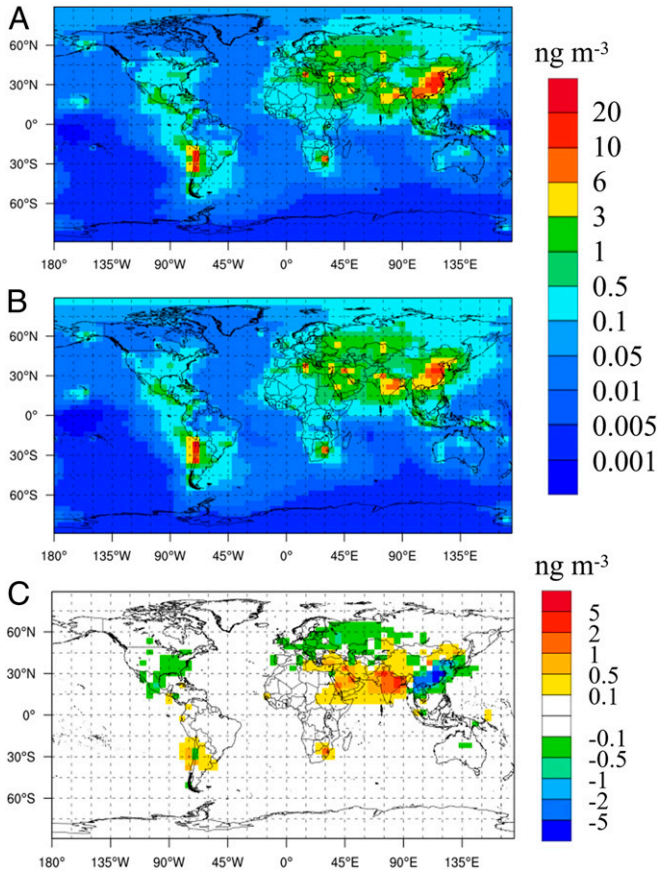

Fig. 2. Spatial distribution of atmospheric arsenic concentration from GEOS-Chem in 2005 (*A*) and 2015 (*B*) and the temporal variation (2015 minus 2005; *C*).

Global Health Risk Assessment of Atmospheric Arsenic via Inhalation Exposure. Based on the global arsenic concentration discussed above, the risk assessment model, detailed in *Materials and Methods*, was applied to quantify the carcinogenic and noncarcinogenic effects from arsenic inhalation in 2005 and 2015. The population was divided into two categories, children and adults, and the carcinogenic effect was determined by CR value, with threshold of 1×10^{-6} (one cancer per million people), recommended by the US EPA (27). The global distribution of CR values for adults and children in 2005 and 2015 is displayed in Fig. 3. There are multiple regions with CR values of adults and children exceeding the threshold, including Asia, Europe, South America, and Africa. Moreover, it is obvious that the CR values exceeding the threshold for adults span much wider areas compared with children, mainly due to the differences in the length of exposure (i.e., 6 y for children and 24 y for adults). In particular, the CR values for adults over eastern China and north-central Chile may reach 10 times as high as the cancer risk threshold in 2005 and 2015 (Fig. 3 *C* and *D*).

Depending on the CR values depicted in Fig. 3, the number of people, living in areas with CR value exceedance of 10^{-6}, was calculated based on the population data from LandScan (https://landscan.ornl.gov/landscan-datasets), shown in Fig. 4. The population is divided into children (15 y old or younger) and adults based on global population age distribution data from the United Nations (https://population.un.org/wpp/Download/Standard/Population).

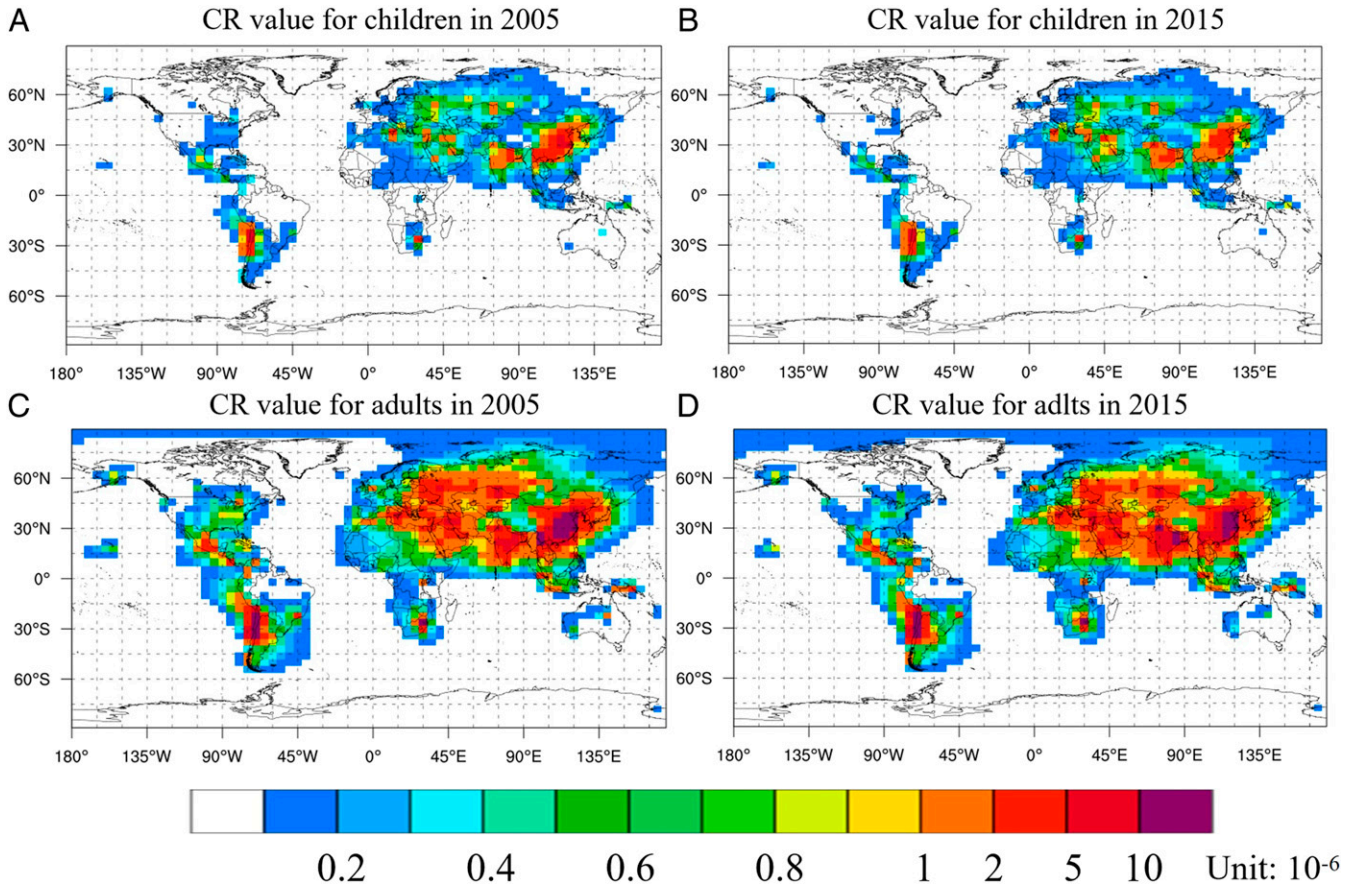

Fig. 3. Spatial distribution of CR value in 2005 for children (*A*) and adults (*B*) and in 2015 for children (*C*) and adults (*D*).

The LandScan data were interpolated to have the same horizontal grid resolution as GEOS-Chem, and the number of people in areas exceeding the CR threshold was added together. The results in Fig. 4 show that 3.55 (2.48 to 4.15, 95% CI based on the Monte Carlo method introduced in *Materials and Methods*) billion and 4.09 (2.80 to 4.65) billion people were living in environments with a CR above the threshold (10^{-6}) globally in 2005 and 2015, respectively. This number accounts for 54% (38 to 64%) and 56% (38 to 64%) of the total population in 2005 and 2015, respectively, of which 0.69 (0.38 to 0.74) billion and 0.66 (0.36 to 0.82) billion were children.

China, India, and Bangladesh rank as the top three countries in numbers exposed to excess cancer risk from atmospheric arsenic inhalation in both 2005 and 2015, a result of a high atmospheric arsenic concentration as well as dense population over these areas. The population, affected by arsenic, increased in 2015 (4.09 billion vs. 3.55 billion in 2005) and was mainly located China, India, Bangladesh, Egypt, Argentina, Chile, and Mexico. It is noteworthy that in 2015, India surpassed China to become the country with the highest number of people, 1.08 (0.76 to 1.25) billion, breathing excessive arsenic levels (i.e., over 80% of its population that year).

This can also be seen in *SI Appendix*, Fig. S12*A*, which shows the number of people affected by atmospheric arsenic in these seven countries. Further analysis through normalization by the total population in the respective country (*SI Appendix*, Fig. S12*B*) shows that the Chilean population has a risk is comparable with the top three countries. In addition to CR health risk, the hazard coefficient (HQ) from noncarcinogenic health risk is displayed in *SI Appendix*, Fig. S13, with details in *SI Appendix*, section 5.

Comparison of Health Risks Due to Arsenic Pollution from Atmosphere and Water. Arsenic pollution in water has long been an issue and has been the subject of much research, but the health impact from atmospheric arsenic has been relatively ignored. To compare the two, all of the literature available with a focus of arsenic health risk from groundwater in a specific site was compiled, and then, the models resulting from the corresponding grid were extracted. The compiled literature results are summarized in *SI Appendix*, Table S3 covering both carcinogenic effects (from 32 sites) and noncarcinogenic effects (from 21 sites) of groundwater arsenic (site locations are shown in *SI Appendix*, Fig. S14). Upon these observations and model results, comparison of CR for adults and noncarcinogenic effect via atmospheric arsenic inhalation is shown in Fig. 5.

Among the 32 sites showing CR, depicted in Fig. 5*A*, 30 sites have a groundwater arsenic problem, leaving only 2 satisfying the threshold (upward-facing triangles in Fig. 5*A*). The health risk assessment, however, indicates that the atmospheric arsenic in all of the 32 sites exceeds the threshold, indicating that beyond the groundwater arsenic issue widely studied previously, the atmospheric arsenic indeed also exerts health risk to the population over these regions. This so-called compound effect resulting from two or more factors (39, 40) may aggravate each other and thereby, result in much more severe impact. Regarding the magnitude, albeit of smaller value from arsenic in atmosphere compared with groundwater, almost half of the sites with arsenic

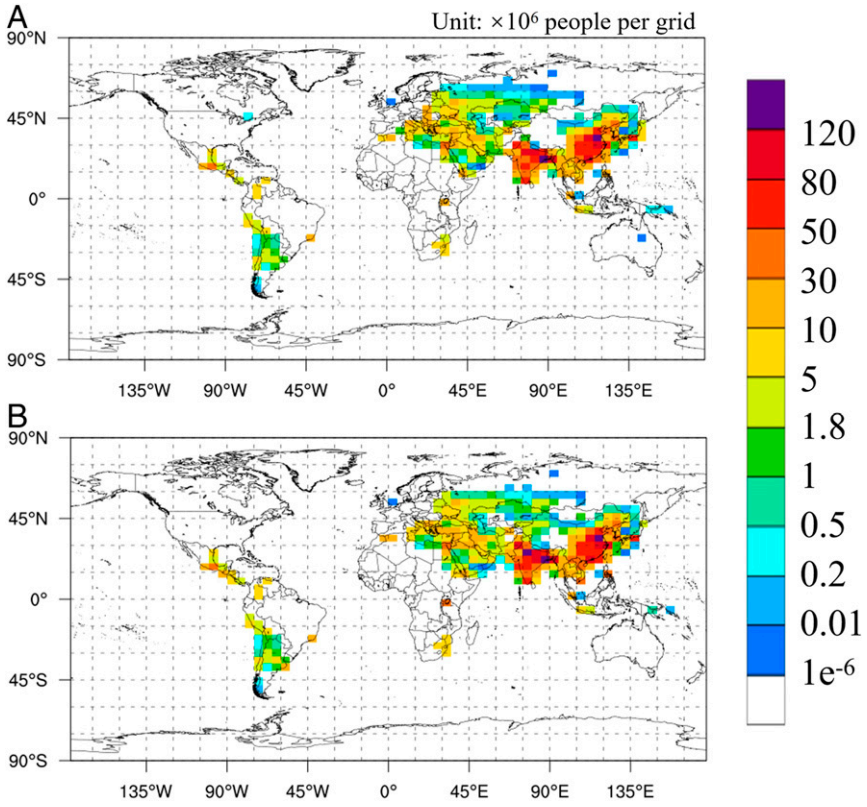

Fig. 4. Population density (in million people per model grid) for people experiencing significant (exceeding 10^{-6}) cancer risk due to atmospheric arsenic inhalation in (*A*) 2005 and (*B*) 2015.

CR from atmosphere exceeded 10% of the value from the groundwater (i.e., central China, India, Thailand, Iran, Pakistan, Cambodia, and Laos). Moreover, a few sites showed even larger atmospheric arsenic exposure in comparison with groundwater (i.e., the values in Subarnarekha River in India, Khyber Pakhtunkhwa in Pakistan, and Dehgolan in Iran are 1.41, 7.92, and 17.9 times as high as the value from groundwater) (Fig. 5*A*).

Regarding the noncarcinogenic effect from arsenic (Fig. 5*B*), most of the sites (a total of 21) showed no exceedance of the criteria of one (41), with the exception of Punjab in Pakistan, Kandal in Cambodia, Melen watershed in Turkey, and two sites of Bangladesh (marked as downward-facing triangles in Fig. 5*B*). By adding the compound effect from atmospheric arsenic, an extra four sites located in India, China, and Vietnam (red diamonds in these countries in Fig. 5*C*) exceed the criteria, almost doubling the number (5) of original sites with exceedance, implicative of the essential significance by taking into account both atmosphere and groundwater.

Please be aware that the abovementioned comparison of arsenic effect is made over atmosphere and groundwater. Indeed, it should be noted that most people drink treated water instead of groundwater directly. For instance, surveys have shown that in Hanan province, Vietnam, more than 87% of households use treated water with removal rate of arsenic as high as 90% (14, 42), and similar process efficiency can also be achieved in Bangladesh (43). If this process of treating groundwater was carried out, the health risks of atmospheric arsenic in many areas (14 of 32 carcinogenic study sites and 17 of 21 noncarcinogenic study sites) may, instead, surpass the health risks from water (*SI Appendix*, Fig. S15). Moreover, the differences of exposure with atmospheric and groundwater arsenic pollution between urban and rural areas are detailed in *SI Appendix*, section 7. This clearly addressed the urgency and necessity of taking the atmospheric arsenic pollution into serious consideration in regard of protecting human beings from health risks due to arsenic.

Discussion

We develop an updated global arsenic emission inventory and implement it into a global model (GEOS-Chem) to simulate the distribution of global atmospheric arsenic concentration and deposition for 2005 and 2015.

Detailed model evaluation using all of the available data from various sources indicates that the model performs reasonably well (Fig. 1 and *SI Appendix*, Fig. S6) and successfully captures the large spatial variations of atmospheric arsenic around the world.

Compared to a previous study on atmospheric arsenic at the global scale (29), this study improved the arsenic emission inventory and also carried out further model evaluation by utilizing more observational data available. Overall, based on comparison of measured vs. modeled results (Fig. 1 and *SI Appendix*, Fig. S6), we achieved reasonable performance with the improved emission inventory.

The distribution of arsenic globally shows large spatial heterogeneity, with high concentrations over Chile, eastern China, and India. A mean arsenic concentration increase of 0.34 ng/m^3 was found in Chile from 2005 to 2015. Over eastern China, the arsenic concentration decreases by 22% from 2005 to 2015 due to stricter air quality regulations. The largest increases (up to 65%) in atmospheric arsenic concentrations during the 2005–2015 period are found over India, where there are already serious issues with particulate air pollution (44).

The combined effect from arsenic in both atmosphere and groundwater may substantially aggravate both the carcinogenic

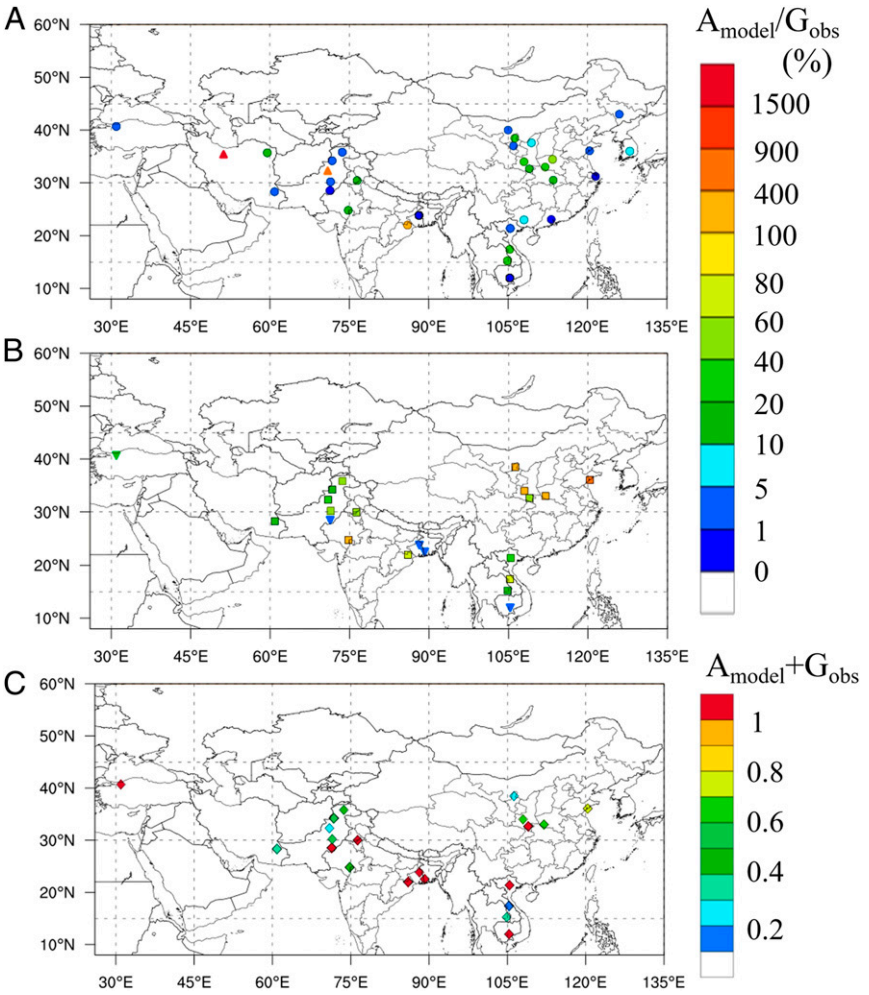

Fig. 5. The ratio of carcinogenic (*A*) and noncarcinogenic (*B*) effect of arsenic in the atmosphere to that in groundwater and the sum of arsenic noncarcinogenic effect from water and atmosphere. In *A*, the upward-facing triangles and circles represent the CR value exceeding the threshold in atmosphere only and both atmosphere and water, respectively. In *B*, the downward-facing triangles represent the HQ value exceeding the criteria in groundwater, whereas the locations without HQ exceedance are marked with squares. In *C*, the diamonds indicate the combined effect by adding the HQ from arsenic in the atmosphere and groundwater. All information about observational sites was acquired from literature described in *SI Appendix*, Fig. S12 and Table S3.

and noncarcinogenic impact on human beings. Although a number of studies have pinpointed arsenic CR from groundwater, this study further illuminates that the atmospheric arsenic CR may exceed the level from groundwater in many parts of the world. This effect is even more obvious for non-CR, for which a single factor, atmospheric arsenic or groundwater arsenic, may not yield an exceedance of health criteria. However, the compound effect then steers the risk to the level higher than the criteria, strongly implying the importance of control strategies in reducing the arsenic in both the atmosphere and groundwater.

Materials and Methods

Model Configuration. A three-dimensional atmospheric chemical transport model GEOS-Chem (v11-02; http://acmg.seas.harvard.edu/geos/) was used to simulate the distribution and evolution of global atmospheric arsenic, which has been used in previous arsenic-related studies (29, 45). The model is driven by the Modern-Era Retrospective analysis for Research and Applications, Version 2 meteorological data with a horizontal resolution of 4° latitude by 5° longitude and 72 vertical layers. The arsenic is considered as an inert tracer added in GEOS-Chem, following Wai et al. (29).

Health Risk Assessment. Exposure to atmospheric arsenic inhalation may lead to carcinogenic and noncarcinogenic health risk via human inhalation, which can be quantified using the CR and HQ, respectively. Both CR and HQ can be determined based on the exposure concentration (EC; micrograms per meter^3), which can be calculated in Eq. **1** (41). After EC is achieved, CR can then be derived by the product of EC and a factor called inhalation unit risk (4.3×10^{-3} μg^{-1} m^3) (46), and HQ is indeed the normalization of EC by inhalation reference concentrations (*RfCi*; 0.5×10^{-2} μg m^{-3}) (46). This assumes that the entire population breathes concentrations equivalent to the ambient levels:

$$EC = CA \times \frac{EF \times ET \times ED}{AT}, \quad [1]$$

where

CA: contaminant concentration in air (micrograms per meter^3; CA is the atmospheric arsenic concentration from GEOS-Chem in this study);

EF: exposure frequency (350 d y^{-1});

ET: exposure time (24 h d^{-1});

ED: exposure duration (6 y for children and 24 y for adults);

AT: averaging time (for carcinogens: AT = 70 y × 365 d × 24 h; for noncarcinogens: AT = ED × 365 d × 24 h).

The same assumption was made for waterborne exposures (i.e., the local population drinks only untreated local groundwater, which is undoubtedly conservative for many populations). All environmental forms of arsenic are included as it is assumed that, in the body, other forms convert quickly to the more toxic arsenic-III (47).

Global Atmospheric Arsenic Emission Inventory. Based on the global atmospheric arsenic emission inventory for 2005 in Wai et al. (29), we substantially improved the inventory for the year 2005 as well as 2015. The emission sources can be in general divided into three major types. First (Type I), the direct arsenic emission inventory is available over regions including the United States, Europe, Japan, Australia, and Canada. Second (Type II), over Chile and China, the arsenic emission was estimated based on the coal combustion, nonferrous metal smelting, etc. Last (Type III), for all of the other regions, the arsenic emissions are estimated based on SO_2 from Emission Database for Global Atmospheric Research (48). More details about the improvement of the emission inventory in 2005 and 2015 are discussed in *SI Appendix*, section 1.

Uncertainty Analysis. Considering the potential uncertainties associated with the emission sources, uncertainties quantifications were applied to carry out the uncertainty of health risk assessment. The Monte Carlo simulation was used for uncertainty analysis. The GEOS-Chem model output results and the input parameters of the health risk model were taken into account. For the uncertainty study of the input parameters of the health risk model, we derived the variation of parameters from the US EPA (49). The 95% CIs are derived from the 50,000 Monte Carlo simulations. Details are presented in *SI Appendix*, section 6.

Data Availability. The data of the paper are available upon request to the corresponding authors.

ACKNOWLEDGMENTS. This research was supported by National Key Project of Ministry of Science and Technology Grant 2017YFC1404101; Shandong Provincial Natural Science Foundation, China Grant ZR2017MD026; and Fundamental Research Funds for the Central Universities Grant 201941006.

1. R. R. Engel, A. H. Smith, Arsenic in drinking water and mortality from vascular disease: An ecologic analysis in 30 counties in the United States. *Arch. Environ. Health* **49**, 418–427 (1994).
2. K. Welch, I. Higgins, M. Oh, C. Burchfiel, Arsenic exposure, smoking, and respiratory cancer in copper smelter workers. *Arch. Environ. Health* **37**, 325–335 (1982).
3. H. S. Yu, W. T. Liao, C. Y. Chai, Arsenic carcinogenesis in the skin. *J. Biomed. Sci.* **13**, 657–666 (2006).
4. European Commission, Air Quality Standards (2013). https://ec.europa.eu/environment/air/quality/standards.htm. Accessed 10 April 2020.
5. WHO, Guidelines for Drinking-water Quality Third Edition Incorporating the First and Second Addenda Volume 1 Recommendations (2008). https://www.who.int/water_sanitation_health/publications/2011/wsh_vol1_1and2_addenda.pdf?ua=1. Accessed 10 April 2020.
6. N. Jiang *et al*., Chemical characteristics and source apportionment of $PM_{2.5}$ between heavily polluted days and other days in Zhengzhou, China. *J. Environ. Sci. (China)* **66**, 188–198 (2018).
7. S. M. Serbula, J. S. Milosavljevic, A. A. Radojevic, J. V. Kalinovic, T. S. Kalinovic, Extreme air pollution with contaminants originating from the mining-metallurgical processes. *Sci. Total Environ.* **586**, 1066–1075 (2017).
8. M. Huang *et al*., Risk assessment of arsenic and other metals via atmospheric particles, and effects of atmospheric exposure and other demographic factors on their accumulations in human scalp hair in urban area of Guangzhou, China. *Ecotoxicol. Environ. Saf.* **102**, 84–92 (2014).
9. D. Chakraborti *et al*., Groundwater arsenic contamination in Bangladesh—21 years of research. *J. Trace Elem. Med. Biol.* **31**, 237–248 (2015).
10. S. A. Moni, G. S. Satter, A. H. M. S. Reza, M. A. Ahsan, Hydrochemistry and arsenic contamination of shallow aquifers in Bidyananda and Nazimkhan Unions, Rajarhat Upazilla, Kurigram, Bangladesh. *J. Geol. Soc. India* **94**, 395–404 (2019).
11. A. H. Hamidian, N. Razeghi, Y. Zhang, M. Yang, Spatial distribution of arsenic in groundwater of Iran, a review. *J. Geochem. Explor.* **201**, 88–98 (2019).
12. W. Ali, A. Rasool, M. Junaid, H. Zhang, A comprehensive review on current status, mechanism, and possible sources of arsenic contamination in groundwater: A global perspective with prominence of Pakistan scenario. *Environ. Geochem. Health* **41**, 737–760 (2019).
13. J. E. Podgorski *et al*., Extensive arsenic contamination in high-pH unconfined aquifers in the Indus Valley. *Sci. Adv.* **3**, e1700935 (2017).
14. T. Agusa *et al*., Human exposure to arsenic from drinking water in Vietnam. *Sci. Total Environ.* **488–489**, 562–569 (2014).
15. P. Li, X. Li, X. Meng, M. Li, Y. Zhang, Appraising groundwater quality and health risks from contamination in a semiarid region of northwest China. *Expo. Health* **8**, 361–379 (2016).
16. J. Chen, H. Qian, H. Wu, Y. Y. Gao, X. Y. Li, Assessment of arsenic and fluoride pollution in groundwater in Dawukou area, Northwest China, and the associated health risk for inhabitants. *Environ. Earth Sci.* **76**, 314 (2017).
17. A. R. M. T. Islam, S.-H. Shen, M. Bodrud-Doza, Assessment of arsenic health risk and source apportionment of groundwater pollutants using multivariate statistical techniques in Chapai-Nawabganj district, Bangladesh. *J. Geol. Soc. India* **90**, 239–248 (2017).
18. M. A. Rahman *et al*., Coliform Bacteria and trace metals in drinking water, southwest Bangladesh: Multivariate and human health risk assessment. *Int. J. Environ. Res.* **13**, 395–408 (2019).
19. V. Duggal, A. Rani, R. Mehra, V. Balaram, Risk assessment of metals from groundwater in northeast Rajasthan. *J. Geol. Soc. India* **90**, 77–84 (2017).
20. K. Ravindra, S. Mor, Distribution and health risk assessment of arsenic and selected heavy metals in Groundwater of Chandigarh, India. *Environ. Pollut.* **250**, 820–830 (2019).
21. M. Radfard *et al*., Drinking water quality and arsenic health risk assessment in Sistan and Baluchestan, Southeastern Province, Iran. *Hum. Ecol. Risk Assess.* **25**, 949–965 (2018).
22. H. Rezaei *et al*., Levels, distributions and health risk assessment of lead, cadmium and arsenic found in drinking groundwater of Dehgolan's villages, Iran. *Toxicol. Environ. Health Sci.* **11**, 54–62 (2019).
23. S. Khan, I. A. Shah, S. Muhammad, R. N. Malik, M. T. Shah, Arsenic and heavy metal concentrations in drinking water in Pakistan and risk assessment: A case study. *Hum. Ecol. Risk Assess.* **21**, 1020–1031 (2014).
24. N. Gul, M. T. Shah, S. Khan, N. U. Khattak, S. Muhammad, Arsenic and heavy metals contamination, risk assessment and their source in drinking water of the Mardan District, Khyber Pakhtunkhwa, Pakistan. *J. Water Health* **13**, 1073–1084 (2015).
25. J. Liu *et al*., Emission control priority of $PM_{2.5}$-bound heavy metals in different seasons: A comprehensive analysis from health risk perspective. *Sci. Total Environ.* **644**, 20–30 (2018).
26. D. Sah, P. K. Verma, K. M. Kumari, A. Lakhani, Chemical fractionation of heavy metals in fine particulate matter and their health risk assessment through inhalation exposure pathway. *Environ. Geochem. Health* **41**, 1445–1458 (2019).
27. US EPA, "Risk Assessment Guidance for Superfund: Volume I Human Health Evaluation Manual (Part B, Development of Risk-Based Preliminary Remediation Goals), Interim, Office of Emergency and Remedial Response" (Rep. EPA/540/R-92/003, US Environmental Protection Agency, 1991).
28. M. Adani, M. Mircea, M. D'Isidoro, M. P. Costa, C. Silibello, Heavy metal modelling study over Italy: Effects of grid resolution, lateral Boundary conditions and foreign emissions on air concentrations. *Water Air Soil Pollut.* **226**, 1–10 (2015).
29. K. M. Wai, S. Wu, X. Li, D. A. Jaffe, K. D. Perry, Global atmospheric transport and source-receptor relationships for arsenic. *Environ. Sci. Technol.* **50**, 3714–3720 (2016).
30. H. Z. Tian *et al*., Trend and characteristics of atmospheric emissions of Hg, As, and Se from coal combustion in China, 1980–2007. *Atmos. Chem. Phys.* **10**, 11905–11919 (2010).
31. C. Zhu, H. Tian, J. Hao, Global anthropogenic atmospheric emission inventory of twelve typical hazardous trace elements, 1995-2012. *Atmos. Environ.* **220**, 1117061 (2020).
32. US EPA, *Guidance on the Use of Models and Other Analyses for Demonstrating Attainment of Air Quality Goals for Ozone, PM2.5, and Regional Haze*, (US Environmental Protection Agency, 2007), p. B-407-002.
33. INN, Investing News Network (INN): Top Copper Production by Country. https://investingnews.com/daily/resource-investing/base-metals-investing/copper-investing/copper-production-country/. Accessed 10 April 2020.
34. H. Tian *et al*., Atmospheric emission inventory of hazardous trace elements from China's coal-fired power plants: Temporal trends and spatial variation characteristics. *Environ. Sci. Technol.* **48**, 3575–3582 (2014).
35. BP, BP Statistical Review of World Energy 2019. https://www.bp.com/en/global/corporate/energy-economics/statistical-review-of-world-energy.html. Accessed 10 April 2020.
36. N. Mirlean, P. Baisch, D. Diniz, Arsenic in groundwater of the Paraiba do Sul delta, Brazil: An atmospheric source? *Sci. Total Environ.* **482–483**, 148–156 (2014).
37. A. H. Smith *et al*., Chronic respiratory symptoms in children following in utero and early life exposure to arsenic in drinking water in Bangladesh. *Int. J. Epidemiol.* **42**, 1077–1086 (2013).
38. W. H. Yu, C. M. Harvey, C. F. Harvey, Arsenic in groundwater in Bangladesh: A geostatistical and epidemiological framework for evaluating health effects and potential remedies. *Water Resour. Res.* **39**, 1146 (2003).
39. J. X. Zhang *et al*., Impacts of compound extreme weather events on ozone in the present and future. *Atmos. Chem. Phys.* **18**, 9861–9877 (2018).
40. J. Zscheischler *et al*., Future climate risk from compound events. *Nat. Clim. Chang.* **8**, 467–477 (2018).
41. US EPA, Risk Assessment Guidance for Superfund (RAGS): Part A. https://www.epa.gov/risk/risk-assessment-guidance-superfund-rags-part. Accessed 10 April 2020.

42. V. A. Nguyen, S. Bang, P. H. Viet, K. W. Kim, Contamination of groundwater and risk assessment for arsenic exposure in Ha Nam province, Vietnam. *Environ. Int.* **35**, 466–472 (2009).
43. J. Q. Jiang, S. M. Ashekuzzaman, A. Jiang, S. M. Sharifuzzaman, S. R. Chowdhury, Arsenic contaminated groundwater and its treatment options in Bangladesh. *Int. J. Environ. Res. Public Health* **10**, 18–46 (2012).
44. S. Chowdhury *et al*., Indian annual ambient air quality standard is achievable by completely mitigating emissions from household sources. *Proc. Natl. Acad. Sci. U.S.A.* **116**, 10711–10716 (2019).
45. J. W. Xu *et al*., Simulation of airborne trace metals in fine particulate matter over North America. *Atmos. Environ.* **214**, 116883 (2019).
46. US EPA, Regional Screening Levels (RSLs)—Generic Tables, US Environmental Protection Agency (US EPA). https://www.epa.gov/risk/regional-screening-levels-rsls-generic-tables. Accessed 10 April 2020.
47. IARC Working Group on the Evaluation of Carcinogenic Risks to Humans, Arsenic, metals, fibres, and dusts. *IARC Monogr. Eval. Carcinog. Risks Hum.* **100**, 11–465 (2012).
48. M. Crippa *et al*., Forty years of improvements in European air quality: Regional policy-industry interactions with global impacts. *Atmos. Chem. Phys.* **16**, 3825–3841 (2016).
49. US EPA, "Exposure Factors Handbook, National Center for Environmental Assessment, Office of Research and Development" (Rep. EPA/600/P-95/002Fa-c, US Environmental Protection Agency, 1997).